scientific reports

Check for updates

OPEN

Clinical implication of aberrant choroidal feeding artery in type 1 macular neovasculopathy

Hyun Seung Yang[1,2,3] & Sohee Jeon[4]✉

Type 1 macular neovascularization (MNV) is the most common type of MNV located in the sub-retinal pigment epithelium (RPE). Although type 1 MNV harbors significant clinical variabilities, the underlying pathomechanism has not been fully elucidated yet. The present study evaluated the characteristics of the choroidal feeding artery in 51 eyes with type 1 MNV using a multimodal imaging composite. In most cases (88.2%), a clear, visible connection between the MNV and choroidal artery was not confirmed. A seamless connection between the MNV and the underlying choroidal feeding artery was found in six of 51 eyes (11.8%). Patients with this aberrant choroidal feeding artery showed large pigment epithelial detachments (PED; $P < 0.001$) and sub-RPE deposits ($P < 0.001$) more frequently. Patients with aberrant choroidal feeding arteries achieved a dry macula of a similar percentage ($P = 0.680$) with more frequent anti-vascular endothelial growth factor injections ($P = 0.005$) and a switch to brolucizumab ($P = 0.042$) during a similar follow-up period ($P = 0.305$). Type 1 MNV with aberrant choroidal feeding arteries showed distinct characteristics from unimpeded blood flow (Large PED and sub-RPE deposits), suggesting that the aberrant choroidal arteries serve not only as a source of blood flow but also contribute to the development of MNV by arteriogenesis.

Keywords Choroidal artery, Indocyanine green angiography, Pachychoroid neovasculopathy, Pigment epithelial detachment, Polypoidal choroidal vasculopathy, Type 1 macular neovascularization

Exudative age-related macular degeneration (AMD) is a progressive degenerative macular disease that leads to visual loss due to macular neovascularization (MNV)[1]. MNVs are divided into three types based on their location and origin[2]. Type 1 MNV, the most common type of MNV, is located in the sub-retinal pigment epithelium (RPE) and harbors significant clinical variabilities[3].

While sharing the exact sub-RPE location, specific patient groups, i.e., pachychoroid neovasculopathy (PNV) and polypoidal choroidal neovasculopathy (PCV), show distinct characteristics, such as less AMD (drusen or subretinal drusenoid deposits) features[4] and lower vascular endothelial growth factor (VEGF) expression[5,6] than other patients with type 1 MNV. Therefore, pachychoroid-driven pathophysiology, including direct compression from pachyvessel, ischemia from venous insufficiency, and primary choriocapillaris loss, has been speculated to be the primary pathophysiology for these patients[7,8]. However, some patients with type 1 MNV have neither AMD nor pachychoroid features, suggesting that there could be a further unknown pathophysiology[9].

Previously, we found that the focal shear stress from the underlying choroidal artery in central serous chorioretinopathy (CSC) may contribute to chronicity and PNV development by breaking Bruch's membrane[10]. In the present study, we evaluated the characteristics of choroidal feeding arteries in eyes with type 1 MNV in the context of a multimodal imaging composite to address whether these characteristics can contribute to the clinical variability of type 1 MNV.

Results

Fifty-one eyes from 51 patients with type 1 MNV were included. In most eyes (n = 45, 88.2%), sub-RPE neovascularization detected in optical coherence tomography-angiography (OCTA; Heidelberg Engineering, Heidelberg, Germany) was located above the choroidal arteries and veins (Fig. 1). In these cases, we could presume that the underlying choroidal arteries would be feeding choroidal arteries. Still, we could not establish an exact relationship between sub-RPE neovascularization and the underlying choroidal arteries. On the other hand, we found six eyes (11.8%) that showed a direct connection between sub-RPE neovascularization and

[1]Department of Ophthalmology, Seoul Shinsegae Eye Center, Seoul, Republic of Korea. [2]Biomedical Imaging Research Institute, Seoul Shinsegae Eye Center, Seoul, Republic of Korea. [3]Department of Applied Bioengineering, Graduate School of Convergence Science and Technology, Seoul National University, Seoul, Republic of Korea. [4]Keye Eye Center, 326 Teheran-ro, Gangnam-gu, Seoul, Republic of Korea. ✉email: soheeeee@gmail.com

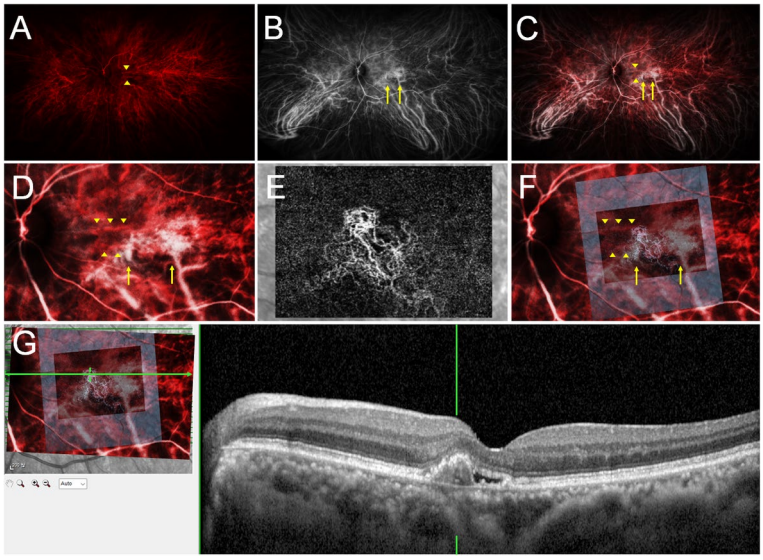

Fig. 1. Representative multimodal imaging composite of a 62-year-old female patient. (**A**) An arterial phase indocyanine green angiography (ICGA) in red revealed two choroidal arteries running horizontally in the macular area (arrowheads). (**B**) A venous phase ICGA revealed choroidal veins running vertically in the macular area (arrows). (**C**) A merged ICGA image showed the location of choroidal arteries (arrowheads) and veins (arrows). (**D**) The enlarged ICGA and (**E**) optical coherence tomography-angiography (OCTA) images were overlapped (**F**) to identify the interrelation between sub-retinal pigment epithelium (RPE) neovascularization and choroidal vessels. Sub-RPE neovascularization was located over choroidal arteries (arrowheads) and veins (arrows) without a definite connection with underlying choroidal vessels. (**G**) A merged image of ICGA, OCTA, and optical coherence tomography revealed that the irregular pigment epithelial detachment consisted of tangled sub-RPE neovascularization.

the choroidal artery (Fig. 2). The choroidal artery in indocyanine green angiography (ICGA; Optos PLC, Dunfermline, UK) continued as the sub-RPE neovascularization in OCTA, and the rest of the vascular network was stained during the venous phase. This seamless continuity between sub-RPE neovascularization and choroidal artery led us to name this choroidal artery an aberrant choroidal feeding artery. More specifically, we diagnosed an aberrant choroidal feeding artery with the following criteria: (1) a choroidal vessel showing fluorescence at the initial flushing of ICGA; (2) then the fluorescence diminished in the venous phase; (3) the connection between sub-RPE neovascularization and the choroidal artery being continuous without acute angle or narrowing the vascular lumen.

Then, we compared the clinical characteristics of patients with and without the aberrant choroidal feeding artery. The clinical characteristics of the enrolled patients are presented in Table 1. No significant differences were detected in age ($P=0.312$), sex distribution ($P=0.168$), systemic disease ($P=0.659$), laterality ($P>0.999$), refractive error ($P=0.225$), initial or last BCVA (best-corrected visual acuity; $P=0.264$ and 0.841), treatment history ($P=0.404$), polypoidal lesion ($P=0.652$), sub-macular hemorrhage ($P>0.999$), initial or last CST ($P=0.410$ and 0.618), and choroidal thickness ($P=0.173$) between groups.

Patients with aberrant choroidal feeding arteries exhibited large PEDs more frequently ($P<0.001$). Four out of six eyes with aberrant choroidal feeding arteries (66.7%) showed a large PED at baseline, while one out of 45 eyes without aberrant choroidal feeding arteries (2.2%) showed it. The sub-RPE deposit was exclusively found in eyes with aberrant choroidal feeding arteries (0.0% in patients without aberrant arteries vs. 50.0% in patients with it: $P<0.001$). Figure 3 shows representative images of patients with the avascular sub-RPE deposit after the resolution of a large PED. An aberrant choroidal feeding artery (empty arrowheads) connected to a large PED (arrowheads) was detected (Fig. 3A). The connected vessel within the PED stained in the venous phase (Fig. 3B). The multimodal imaging composite revealed that the sub-RPE neovascularization was overlapped with aberrant choroidal feeding artery (Fig. 3C–F). The horizontal and vertical OCTA images showed flow signal crossing at the margin of PED, suggesting that this represents the connection between the aberrant choroidal feeding artery and MNV (Fig. 3G–I). The avascular sub-RPE deposit typically develops after the resolution of a large PED and persists as long as disease activity is maintained (Fig. 3J–N; arrowheads). However, unlike the fibrovascular membrane, the avascular sub-RPE deposit diminished eventually as the disease was inactivated with intravitreal anti-VEGF injections (Fig. 3O; arrowheads).

Dry macular was achieved with a comparable frequency (60.0% for patients without an aberrant artery vs. 50.0% for patients with it; $P=0.680$). However, patients with aberrant choroidal feeding arteries required more frequent injections (16.17 ± 7.33 times) than those without (8.22 ± 6.11 times, $P=0.005$) within a similar follow-up time (33.47 ± 20.98 months for patients without aberrant arteries vs. 42.83 ± 18.97 months for patients with it; $P=0.305$). In addition, a switch to brolucizumab (6.0 mg/0.05 mL; Beovu, Novartis, Basel, Switzerland) was

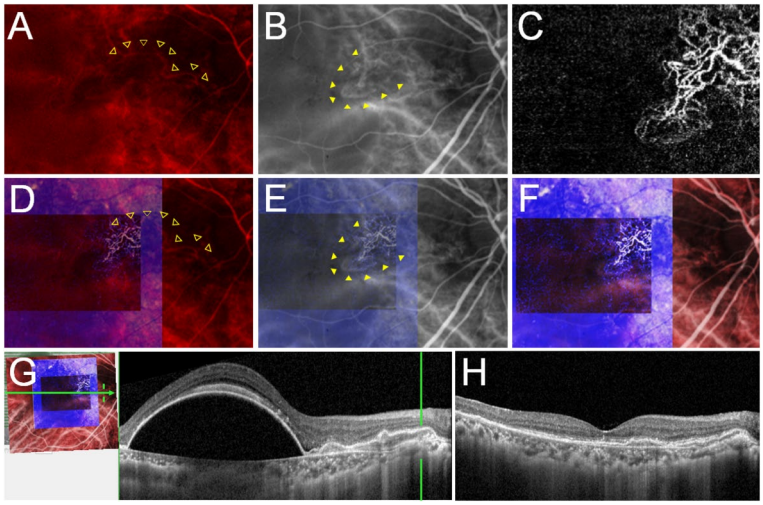

Fig. 2. Representative multimodal imaging composite of a 73-year-old female patient with an aberrant choroidal feeding artery. (**A**) An arterial phase indocyanine green angiography (ICGA) in red showed a choroidal artery running from the peripapillary area (blank arrowheads). (**B**) A venous phase ICGA shows fern-shaped fluorescence (arrowheads). (**C**) The optical coherence tomography-angiography (OCTA) shows sub-retinal pigment epithelium (RPE) neovascularization. (**D**) A merged image showed a direct connection between the choroidal artery in ICGA and sub-RPE neovascularization in OCTA (blank arrowheads). (**E**) A merged image showed a matched location between fern-shaped fluorescence in venous ICGA and sub-RPE neovascularization in OCTA (arrows). (**F**) A merged image of ICGA and OCTA revealed that the sub-RPE neovascularization is directly connected with a choroidal artery and stained in the venous phase in ICGA. (**G**) A multimodal imaging composite suggests the feeding choroidal artery was located between RPE and Bruch's membrane from the peripapillary area. (**H**) The large pigment epithelial detachment was resolved after three consecutive aflibercept injections.

Parameter	No aberrant choroidal arteries (n = 45)	Aberrant choroidal arteries (n = 6)	*P*-value
Age, years	61.9 ± 8.7	65.7 ± 5.8	0.312
Sex, male (%)	31 (68.9)	2 (33.3)	0.168
Systemic disease, yes (%)	16 (35.6)	3 (50.0)	0.659
Laterality, OD (%)	24 (53.3)	3 (50.0)	> 0.999
Refractive error, diopters	− 0.21 ± 2.01	0.83 ± 1.11	0.225
Initial BCVA, LogMAR	0.24 ± 0.24	0.35 ± 0.19	0.264
Last BCVA, LogMAR	0.14 ± 0.17	0.15 ± 0.12	0.841
Treatment naïve, yes (%)	42 (93.3)	5 (83.3)	0.404
Polypoidal lesion, yes (%)	15 (33.3)	3 (50.0)	0.652
Large PED, yes (%)	1 (2.2)	4 (66.7)	< 0.001
Sub-RPE deposit, yes (%)	0 (0.0)	3 (50.0)	< 0.001
Sub-macular hemorrhage, yes (%)	2 (4.4)	0 (0.0)	> 0.999
Initial CST, μm	366.58 ± 87.00	436.67 ± 189.28	0.410
Last CST, μm	278.64 ± 65.58	254.50 ± 109.41	0.618
Choroidal thickness, μm	385.89 ± 121.99	314.67 ± 83.59	0.173
Follow-up period, months	33.47 ± 20.98	42.83 ± 18.97	0.305
Number of injections, times	8.22 ± 6.11	16.17 ± 7.33	0.005
Switch to brolucizumab, yes (%)	5 (11.1)	3 (50.0)	0.042
Dry macula, yes (%)	27 (60.0)	3 (50.0)	0.680

Table 1. Clinical characteristics of enrolled patients (n = 51). *BCVA* best-corrected visual acuity, *CST* central subfield thickness, *PED* pigment epithelial detachment, *RPE* retinal pigment epithelium.

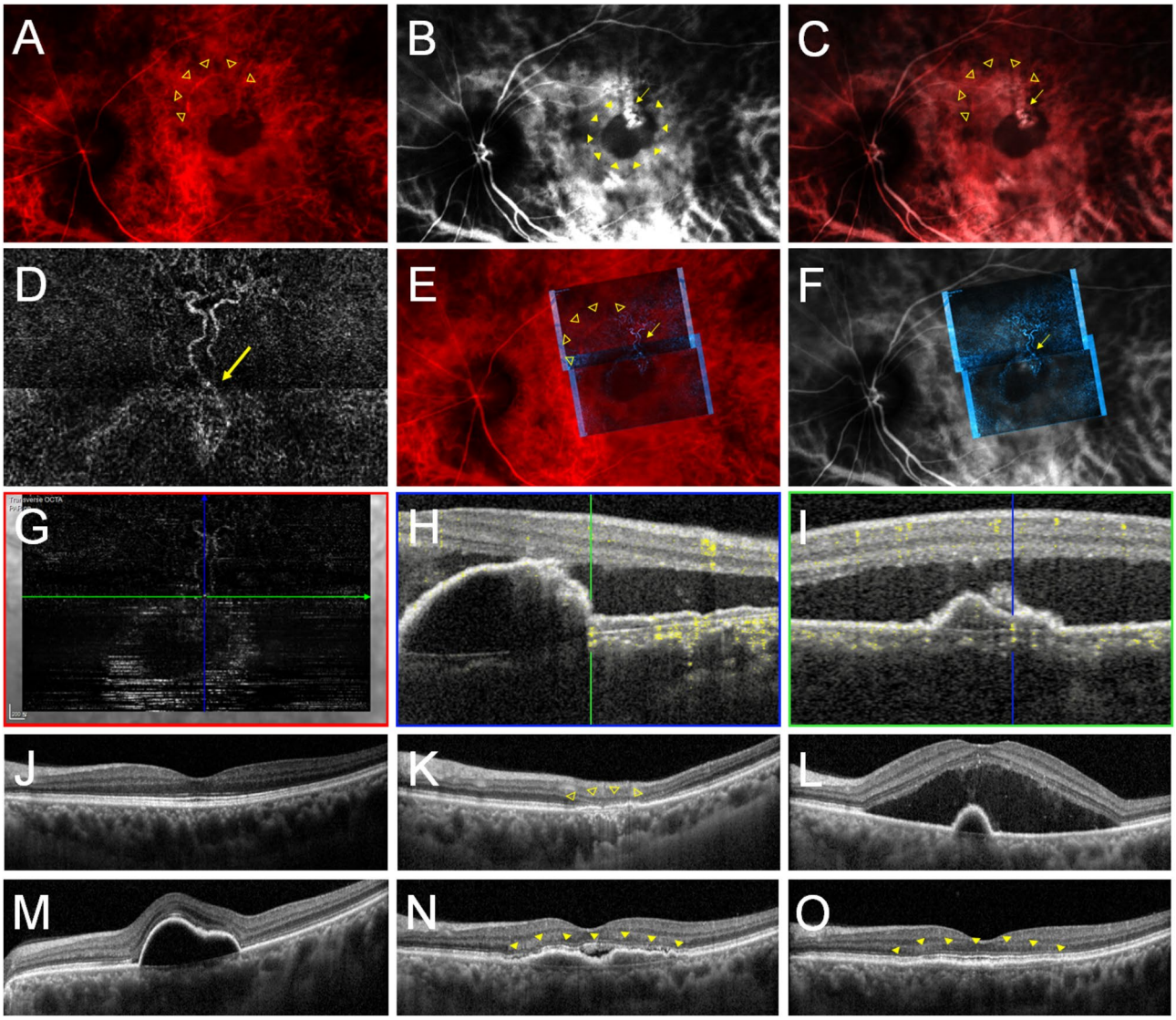

Fig. 3. Representative multimodal imaging composite of a 65-year-old male patient with type 1 macular neovascularization (MNV) exhibiting an aberrant choroidal feeding artery and avascular sub-retinal pigment epithelium (RPE) deposit. (**A**) Arterial phase indocyanine green angiography (ICGA) image showed a choroidal feeding artery (blank arrowheads) larger than retinal vessels that run into the pigment epithelial detachment (PED) area (arrowheads). (**B**) Venous phase ICGA showed a nodular hyperfluorescence (arrow) in the PED area (arrowheads). (**C**) Merged arterial and venous phase ICGA image showed a direct connection between the choroidal feeding artery (blank arrowheads) and a nodular hyperfluorescence (arrow) at the marginal area of PED. (**D**) An optical coherence tomography-angiography (OCTA) image showed sub-RPE neovascularization with tangled vasculature at the end (arrow). (**E**) A merged image of an arterial phase ICGA and OCTA showed partial overlap between a choroidal feeding artery (blank arrowheads) and sub-RPE neovascularization (arrow). (**F**) A merged image of a venous phase ICGA and OCTA showed colocalization of tangled vasculature in OCTA and nodular hyperfluorescence in ICGA (arrow). (**G**) At the margin of PED, flow signal representing the breakage site (arrow) was detected in the (**H**) vertical and (**I**) horizontal OCTA image. (**J**) Before the symptom development, optical coherence tomography (OCT) showed normal fovea and (**K**) flat irregular PED (blank arrowheads). (**L**) A large amount of subretinal fluid (SRF) with PED was detected at the time of symptom development. (**M**) After 1 year of bimonthly aflibercept injections, PED persisted with intermittent SRF development. (**N**) PED decreased with monthly aflibercept injections, but sub-RPE deposits developed and persisted for more than a year (arrowheads). (**O**) Eventually, we changed to brolucizumab as the visual acuity decreased even after a year of monthly aflibercept injections. After two bimonthly brolucizumab injections, the sub-RPE deposit decreased significantly with improved visual acuity (arrowheads).

more frequently required in patients with aberrant choroidal feeding arteries (50.0%) compared to those without (11.1%; $P = 0.042$).

Discussion

Using a multimodal imaging composite, we could evaluate the characteristics of the choroidal feeding artery in type 1 MNV. While there is a high possibility that choroidal arteries are involved in the pathogenesis of type 1 MNV, they have not been thoroughly evaluated. In most eyes with type 1 MNV, sub-RPE neovascularization is located above the choroidal arteries without a clear connection, suggesting that the pathogenesis of these MNV is angiogenesis from underlying choroidal arteries. On the other hand, six out of 51 patients with type 1 MNV (11.8%) exhibited aberrant choroidal feeding arteries that seamlessly connected with sub-RPE neovascularization, suggesting that the pathogenesis of these MNVs may be driven by arteriogenesis from connected choroidal arteries rather than angiogenesis.

We speculate that the aberrant choroidal feeding arteries could contribute to type 1 MNV by the following mechanisms. First, the constant and high flow from the choroidal artery to the sub-RPE neovascularization would contribute to the arteriogenesis of preexisting vessels[11]. Second, shear stress from the choroidal arteries may contribute to the breakage of Bruch's membrane, as we found in the eyes with PNV from CSC[10]. Third, aberrant choroidal arteries directly delivering oxygenated blood flow to the MNV without passing the choriocapillaris might aggravate ischemic damage to the overlying retinal layer, thus triggering further angiogenesis.

The presence of feeder and draining vessels has been researched for patients with PCV[12]. PCV eyes with feeder and draining vessels showed thin choroids; therefore, different pathomechanisms were proposed for these eyes[12]. In the present study, we could not find a significant relationship between aberrant choroidal arteries and polypoidal lesions. We speculate that arteriogenesis is a universal pathomechanism for type 1 MNV, regardless of the presence of polypoidal lesions. Instead, patients with aberrant choroidal feeding arteries showed large PEDs and sub-RPE deposits, suggesting relentless blood inflow from these arteries.

Half of the patients with aberrant choroidal feeding arteries did not respond to aflibercept (2.0 mg/0.05 mL; Eylea, Regeneron, Tarrytown, NY) injections. They required twice as many frequent anti-VEGF injections as the patients without an aberrant choroidal feeding artery. Additionally, patients with aberrant choroidal feeding arteries showed better response to brolucizumab than to aflibercept. Their refractoriness to anti-VEGF is in line with previous studies on large PEDs, which have shown resistance to anti-VEGF treatment[13,14]. The superior anatomic outcome of brolucizumab over aflibercept has been reported previously[15], potentially due to its smaller molecular weight, which allows for a higher drug concentration[16]. Patients with aberrant choroidal feeding arteries may require more potent anti-VEGF treatment that can penetrate the RPE and suppress permeability from MNV that is connected with aberrant choroidal feeding arteries. In addition, contrary to angiogenesis, arteriogenesis is VEGF-independent[17,18], suggesting that arteriogenesis can progress even with anti-VEGF treatment. A comparison of treatment effects from various anti-VEGF injections and photodynamic therapy (PDT) in patients with aberrant choroidal feeding arteries would be desirable in future studies.

Despite the significant difference in the response to the aflibercept injections, the final BCVA was comparable between groups. The prognosis of type 1 MNV depends on multiple factors, including local tissue hypoxia, adjacent RPE dysfunction, the formation of a draining pathway to the choroidal space, and blood flow velocity within the MNV from choroidal arteries. Although ICGA is not a routine examination for patients with AMD in many practices, it might be helpful for patients with type 1 MNV who show signs of abnormal choroidal features.

Our study has several limitations, including a retrospective design and a small sample size. Since the sensitivity in detecting neovascular networks varies significantly depending on the specific OCTA technologies used[19]. The detection rate of aberrant choroidal feeding arteries connected to sub-RPE neovascularization may differ according to the specific OCTA devices. Further study involving a large patient number is required to confirm our preliminary findings. We were unable to measure the exact blood flow velocity using a conventional ICGA imaging system[20]. Studies using advanced imaging systems, such as Doppler OCT[21], are required to enhance our understanding of the role of choroidal arteries in patients with type 1 MNV.

Methods

A retrospective chart review was conducted in patients diagnosed with type 1 MNV who were followed up for more than 6 months between January 2021 and December 2023 at the KEYE Eye Center. Patients with a history of intraocular disease, surgery, focal laser photocoagulation, PDT, any opacity that hindered choroidal imaging, BCVA worse than 0.7 LogMAR that hampered fixation during ocular imaging, or evidence of chronic CSC, type 2 or 3 MNV at any visit were excluded from the study. Patients who received intravitreal anti-VEGF injections within 6 months were also excluded. When two eyes from the same patient were eligible, the eye with a more extensive disease history was selected. The Institutional Review Board (IRB) and Ethics Committee of the KEYE Eye Center approved this study (approval number: P12362378-001). The requirement for informed consent was waived by the IRB and Ethics Committee of the KEYE Eye Center due to the study's retrospective nature. The study protocol was conducted in accordance with the Declaration of Helsinki.

Imaging methods

A multimodal imaging composite was created using the arterial and venous phases of ICGA, OCT, and OCTA images to determine the spatial relationship between choroidal arteries, veins, and MNV, as previously described[10]. An arterial phase ICGA was defined as the first or second ICGA image showing only arterial staining, excluding images showing venous flow. A venous ICGA was taken at the middle phase after maximal staining of the vortex vein to minimize the influence of remnant arterial flow[22]. Discrimination between a choroidal artery and a vein was done by tracing the Vortex vein. Figure 1 illustrates the sequential steps for creating a multimodal

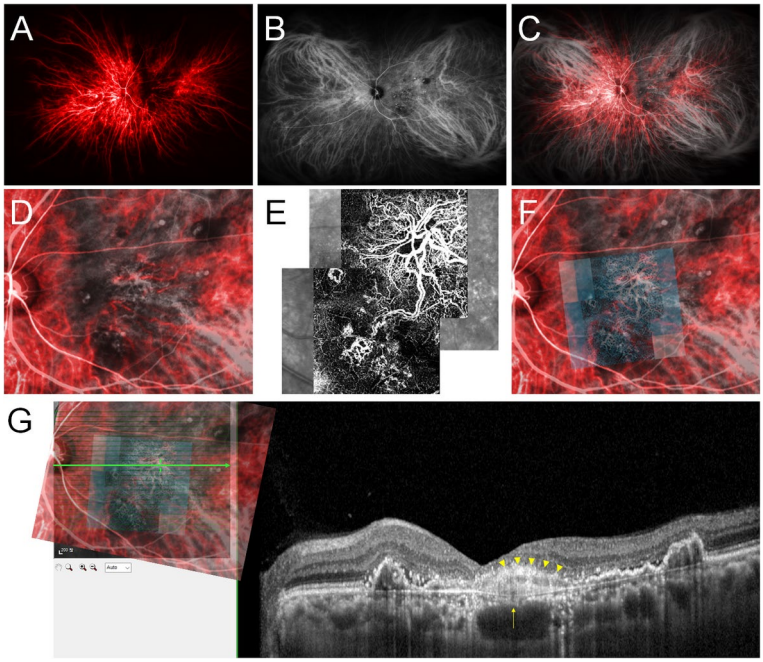

Fig. 4. Sequential steps for making a multimodal imaging composite from a 59-year-old male patient with aneurysmal type 1 macular neovascularization (MNV), also known as polypoidal choroidal vasculopathy. (**A**) An arterial phase indocyanine green angiography (ICGA) in red showed reduced fluorescence in the macular area. (**B**) A venous phase ICGA showed multiple nodular hyperfluorescence, suggesting polypoidal lesions. (**C**) The arterial and venous phase ICGA images were merged by aligning the optic nerve head and retinal arteries. (**D**) The enlarged image showed scattered polypoidal lesions and choroidal arteries in the macular area. (**E**) The optical coherence tomography-angiography (OCTA) showed sub-retinal pigment epithelium (RPE) neovascularization exhibiting a branching vascular network (BVN) and tangled vasculatures. (**F**) Merging the ICGA and OCTA images revealed that the type 1 MNV was located over the choroidal arteries. The tangled vasculatures in OCTA matched the nodular hyperfluorescence in ICGA. (**G**) Merging ICGA, OCTA, and optical coherence tomography images showed BVN (arrowheads) and potential vascular connection through Bruch's membrane breakage (arrow).

imaging composite from arterial and venous ICGA, OCT, and OCTA images using Photoshop (version 21.1.3; Adobe, Inc., San Jose, CA, USA). An arterial ICGA image was colorized red, and the transparency was set at 60% (Fig. 4A). The colored arterial image was superimposed over the venous image (Fig. 4B) by aligning anatomic landmarks (Fig. 4C). Then, the avascular layer of the OCTA image overlapped with the ICGA image (Fig. 4D–F). Finally, the ICGA-OCTA composite was overlaid on the OCT image to correlate with the cross-sectional images (Fig. 4G).

Clinical evaluation

Demographics, initial and final best-corrected visual acuity (BCVA), number of intravitreal anti-VEGF injections, follow-up period, and achievement of a dry macula were collected from electronic medical records. Decimal BCVA values were collected and converted into a logMAR scale for statistical analysis. Our standard treatment protocol for managing MNV involves 3 monthly injections of aflibercept, followed by maintenance using a treat-and-extend (TNE) regimen. However, whether to administer the initial three treatments of aflibercept for type 1 MNV was left to the discretion of the physicians, due to the high clinical variability of the disease. The TNE was extended or shortened by 2 weeks according to the OCT findings. The reinjection criteria were the presence of intraretinal fluid (IRF) or subretinal fluid (SRF) on the OCT image. The PED without IRF or SRF was not regarded as a reinjection criterion, unless it was a large PED that affects visual quality. In cases where complete intraretinal or subretinal fluid resolution was not achieved after 1 year of bimonthly aflibercept treatment, the treatment protocol was modified to monthly aflibercept. Intractable patients who did not respond to monthly aflibercept were switched to brolucizumab as soon as the medication became available in Korea. When the TNE interval was extended to 16 weeks, the injection was suspended, and the patient was followed up regularly at the doctor's discretion. Dry macular was defined as a condition where the fluid-free period lasted longer than 6 months without anti-VEGF treatment.

We collected imaging characteristics, such as the presence of polypoidal lesions[23], large PED (with a minimum greatest linear width of 500 μm and a minimum height of 100 μm)[13,14], avascular sub-RPE deposits, sub-RPE hemorrhage, initial and last central subfield thickness (CST), and choroidal thickness. An avascular sub-RPE deposit was defined as a homogenous material with medium signal intensity, thicker than 150 μm between Bruch's membrane and RPE. The avascularity was confirmed with OCTA.

Statistical analysis

Statistical analyses were performed using SPSS (version 27.0; IBM Corp., Armonk, NY). Descriptive data were recorded as the mean ± standard deviation unless otherwise specified. Independent *t*-tests were used to assess between-group differences in demographic and ocular characteristics. Categorical variables were compared using the chi-square test. Statistical significance was set at $P < 0.05$.

Data availability

The datasets generated and analyzed during the current study are not publicly available due to privacy concerns and regulations regarding patient data protection. However, de-identified data are available from the corresponding author upon reasonable request and with appropriate institutional review board approval.

Received: 19 January 2025; Accepted: 2 May 2025
Published online: 07 May 2025

References

1. Kuehlewein, L. et al. Optical coherence tomography angiography of type 1 neovascularization in age-related macular degeneration. *Am. J. Ophthalmol.* **160**, 739–748 (2015).
2. Spaide, R. F. et al. Consensus nomenclature for reporting neovascular age-related macular degeneration data: consensus on neovascular age-related macular degeneration nomenclature study group. *Ophthalmology* **127**, 616–636 (2020).
3. Jung, J. J. et al. The incidence of neovascular subtypes in newly diagnosed neovascular age-related macular degeneration. *Am. J. Ophthalmol.* **158**, 769–779 (2014).
4. Muth, D. R. et al. Correlation between macular neovascularization (MNV) type and druse type in neovascular age-related macular degeneration (AMD) based on the CONAN classification. *Biomedicines.* **10**, 2370 (2022).
5. Nakashizuka, H. et al. Clinicopathologic findings in polypoidal choroidal vasculopathy. *Invest. Ophthalmol. Vis. Sci.* **49**, 4729–4737 (2008).
6. Tong, J. P. et al. Aqueous humor levels of vascular endothelial growth factor and pigment epithelium-derived factor in polypoidal choroidal vasculopathy and choroidal neovascularization. *Am. J. Ophthalmol.* **141**, 456–462 (2006).
7. Balaratnasingam, C. et al. Polypoidal choroidal vasculopathy: A distinct disease or manifestation of many?. *Retina* **36**, 1–8 (2016).
8. Kuranami, A., Maruko, R., Maruko, I., Hasegawa, T. & Iida, T. Pachychoroid neovasculopathy has clinical properties that differ from conventional neovascular age-related macular degeneration. *Sci. Rep.* **13**, 7379 (2023).
9. van Dijk, E. H. C. et al. The spectrum of polypoidal choroidal vasculopathy in Caucasians: Clinical characteristics and proposal of a classification. *Graefes Arch. Clin. Exp. Ophthalmol.* **259**, 351–361 (2021).
10. Tuuminen, R. & Jeon, S. Choroidal arterial abnormality in central serous chorioretinopathy. *Graefes Arch. Clin. Exp. Ophthalmol.* **262**, 3465–3473 (2024).
11. Spaide, R. F. Optical coherence tomography angiography signs of vascular abnormalization with antiangiogenic therapy for choroidal neovascularization. *Am. J. Ophthalmol.* **160**, 6–16 (2015).
12. Kawamura, A., Yuzawa, M., Mori, R., Haruyama, M. & Tanaka, K. Indocyanine green angiographic and optical coherence tomographic findings support classification of polypoidal choroidal vasculopathy into two types. *Acta Ophthalmol.* **91**, e474–e481 (2013).
13. Tan, A. C. S., Simhaee, D., Balaratnasingam, C., Dansingani, K. K. & Yannuzzi, L. A. A perspective on the nature and frequency of pigment epithelial detachments. *Am. J. Ophthalmol.* **172**, 13–27 (2016).
14. Schmidt-Erfurth, U., Waldstein, S. M., Deak, G. G., Kundi, M. & Simader, C. Pigment epithelial detachment followed by retinal cystoid degeneration leads to vision loss in treatment of neovascular age-related macular degeneration. *Ophthalmology* **122**, 822–832 (2015).
15. Dugel, P. U. et al. HAWK and HARRIER: Ninety-six-week outcomes from the phase 3 trials of brolucizumab for neovascular age-related macular degeneration. *Ophthalmology* **128**, 89–99 (2021).
16. Dugel, P. U. et al. Brolucizumab versus aflibercept in participants with neovascular age-related macular degeneration: A randomized trial. *Ophthalmology* **124**, 1296–1304 (2017).
17. Deindl, E. et al. Role of ischemia and of hypoxia-inducible genes in arteriogenesis after femoral artery occlusion in the rabbit. *Circ. Res.* **89**, 779–786 (2001).
18. Schierling, W. et al. The role of angiogenic growth factors in arteriogenesis. *J. Vasc. Res.* **46**, 365–374 (2009).
19. Mastropasqua, R. et al. Optical coherence tomography angiography in macular neovascularization: A comparison between different OCTA devices. *Transl. Vis. Sci. Technol.* **9**, 6 (2020).
20. Yannuzzi, L. A., Slakter, J. S., Sorenson, J. A., Guyer, D. R. & Orlock, D. A. Digital indocyanine green videoangiography and choroidal neovascularization. *Retina* **12**, 191–223 (1992).
21. Miura, M., Makita, S., Iwasaki, T. & Yasuno, Y. An approach to measure blood flow in single choroidal vessel using Doppler optical coherence tomography. *Invest. Ophthalmol. Vis. Sci.* **53**, 7137–7141 (2012).
22. Dzurinko, V. L., Gurwood, A. S. & Price, J. R. Intravenous and indocyanine green angiography. *Optometry* **75**, 743–755 (2024).
23. Cheung, C. M. G. et al. polypoidal choroidal vasculopathy: Consensus nomenclature and non-indocyanine green angiograph diagnostic criteria from the Asia-pacific ocular imaging society PCV workgroup. *Ophthalmology* **128**, 443–452 (2021).

Author contributions

HK and SJ wrote the main manuscript text and prepared figures. All authors reviewed the manuscript.

Declarations

Competing interests

The authors declare no competing interests.

Additional information

Correspondence and requests for materials should be addressed to S.J.

Reprints and permissions information is available at www.nature.com/reprints.